arXiv:1211.3744v1 [astro-ph.SR] 15 Nov 2012

Direct Imaging Discovery of a 'Super-Jupiter' Around the late B-Type Star κ And*

J. Carson[1,2], C. Thalmann[3,2], M. Janson[4], T. Kozakis[1], M. Bonnefoy[2], B. Biller[2], J. Schlieder[2], T. Currie[5], M. McElwain[5], M. Goto[6], T. Henning[2], W. Brandner[2], M. Feldt[2], R. Kandori[7], M. Kuzuhara[7,8], L. Stevens[1], P. Wong[1], K. Gainey[1], M. Fukagawa[9], Y. Kuwada[9], T. Brandt[4], J. Kwon[7], L. Abe[10], S. Egner[11], C. Grady[5], O. Guyon[11], J. Hashimoto[7], Y. Hayano[11], M. Hayashi[7], S. Hayashi[11], K. Hodapp[12], M. Ishii[11], M. Iye[7], G. Knapp[4], T. Kudo[11], N. Kusakabe[7], T. Matsuo[13], S. Miyama[14], J. Morino[7], A. Moro-Martin[15], T. Nishimura[11], T. Pyo[11], E. Serabyn[16], H. Suto[7], R. Suzuki[7], M. Takami[17], N. Takato[11], H. Terada[11], D. Tomono[11], E. Turner[4,18], M. Watanabe[19], J. Wisniewski[20], T. Yamada[21], H. Takami[7], T. Usuda[11], M. Tamura[7]

⋆Based on data collected at Subaru Telescope, which is operated by the National Astronomical Observatory of Japan.

[1]Department of Physics & Astronomy, College of Charleston, 58 Coming St., Charleston, SC 29424, USA

[2]Max Planck Institute for Astronomy, Heidelberg, Germany

[3]Astronomical Institute "Anton Pannekoek", University of Amsterdam, Science Park 904, 1098 XH Amsterdam, The Netherlands

[4]Department of Astrophysical Sciences, Princeton University, NJ 08544, USA

[5]ExoPlanets and Stellar Astrophysics Laboratory, Code 667, Goddard Space Flight Center, Greenbelt, MD 20771, USA

[6]Universitäts-Sternwarte München, Ludwig-Maximilians-Universität, 81679 München, Germany

[7]National Astronomical Observatory of Japan, 2-21-1 Osawa, Mitaka, Tokyo 181-8588, Japan

[8]Department of Earth and Planetary Science, The University of Tokyo, 7-3-1, Hongo, Bunkyo-ku, Tokyo 113-0033, Japan

[9]Department of Earth and Space Science, Graduate School of Science, Osaka University, 1-1 Machikaneyama, Toyonaka, Osaka 560-0043 Japan

[10]Laboratoire Lagrange (UMR 7293), Universite de Nice-Sophia Antipolis, CNRS, Observatoire de la Cote dAzur, 28 avenue Valrose, 06108 Nice Cedex 2, France

[11]Subaru Telescope, 650 North Aohoku Place, Hilo, HI 96720, USA

[12]Institute for Astronomy, University of Hawaii, 640 N. Aohoku Place, Hilo, HI 96720, USA

[13]Department of Astronomy, Kyoto University, Kitashirakawa-Oiwake-cho, Sakyo-ku, Kyoto, Kyoto 606-8502, Japan

[14]Hiroshima University, 1-3-2, Kagamiyama, Higashihiroshima, Hiroshima 739-8511,

Received _____; accepted _____

Accepted for publication in Astrophysical Journal Letters.

Japan

[15]Departamento de Astrofísica, CAB (INTA-CSIC), Instituto Nacional Técnica Aeroespacial, Torrejón de Ardoz, 28850, Madrid, Spain

[16]Jet Propulsion Laboratory, California Institute of Technology, Pasadena, CA, 171-113, USA

[17]Institute of Astronomy and Astrophysics, Academia Sinica, P.O. Box 23-141, Taipei 10617, Taiwan

[18]Kavli Institute for Physics and Mathematics of the Universe, The University of Tokyo, 5-1-5, Kashiwanoha, Kashiwa, Chiba 277-8568, Japan

[19]Department of Cosmosciences, Hokkaido University, Kita-ku, Sapporo, Hokkaido 060-0810, Japan

[20]HL Dodge Department of Physics & Astronomy, University of Oklahoma, 440 W Brooks St, Norman, OK 73019 USA

[21]Astronomical Institute, Tohoku University, Aoba-ku, Sendai, Miyagi 980-8578, Japan

ABSTRACT

We present the direct imaging discovery of an extrasolar planet, or possible low-mass brown dwarf, at a projected separation of 55 ± 2 AU ($1\farcs058 \pm 0\farcs007$) from the B9-type star κ And. The planet was detected with Subaru/HiCIAO during the SEEDS survey, and confirmed as a bound companion via common proper motion measurements. Observed near-infrared magnitudes of $J = 16.3 \pm 0.3$, $H = 15.2 \pm 0.2$, $K_s = 14.6 \pm 0.4$, and $L' = 13.12 \pm 0.09$ indicate a temperature of ∼1700 K. The galactic kinematics of the host star are consistent with membership in the Columba association, implying a corresponding age of 30^{+20}_{-10} Myr. The system age, combined with the companion photometry, points to a model-dependent companion mass ∼12.8 $M_{\rm Jup}$. The host star's estimated mass of 2.4–2.5 $M_\odot$ places it among the most massive stars ever known to harbor an extrasolar planet or low-mass brown dwarf. While the mass of the companion is close to the deuterium burning limit, its mass ratio, orbital separation, and likely planet-like formation scenario imply that it may be best defined as a 'Super-Jupiter' with properties similar to other recently discovered companions to massive stars.

Subject headings: planets and satellites: detection — stars: massive — brown dwarfs

1. Introduction

Stellar mass is emerging as one of the most important parameters in determining the properties of planetary systems, along with stellar metallicity. Radial velocity surveys have indicated that the frequency of giant planets increases with the mass of the stellar host (Johnson et al. 2010), and many of the roughly dozen exoplanets that have been directly imaged so far have had A-type stellar hosts (e.g., Marois et al. 2008; Lagrange et al. 2009), despite such large stars being in the small minority of surveyed targets. These results have motivated targeted imaging surveys for planets around massive stars (e.g., Janson et al. 2011b). The increase in planet frequency with host star mass can be readily explained theoretically, through the consideration that more massive stars are likely to have more massive disks (Mordasini et al. 2012). On the other hand, massive stars also feature an increased intensity of high-energy radiation, which may significantly shorten the disk lifetime due to photoevaporation, and thus decrease the time window in which giant planets are allowed to form. This raises the question whether there is a maximum stellar mass above which giant planets are unable to form.

In this Letter, we report the discovery of a $\sim$12.8 $M_{\rm Jup}$ companion to the $\sim$2.5 $M_{\odot}$ star κ And, the most massive star to host a directly detected companion below or near the planetary mass limit. In the following, we describe the acquisition, reduction and analysis of the data used for detection, confirmation, and basic characterization of the companion, κ And b.

2. Observations and Data Reduction

Observations of the κ And system extended over a period of seven months (January - July 2012) and were carried out on Subaru Telescope. JHK images were collected with

AO188 (Hayano et al. 2010) coupled with HiCIAO (Hodapp et al. 2008). L' measurements were carried out with AO188 coupled with the Infrared Camera and Spectrograph (IRCS; Tokunaga et al. 1998). Figure 1 displays the multi-wavelength images of the newly discovered companion. Table 1 provides a summary of the experimental measurements, as well as relevant values from the literature. Figure 2 shows observed astrometric positions of κ And b as compared with expected motion of an unrelated background star. The sub-sections below describe the observations in greater detail.

2.1. Subaru HiCIAO/AO188 JHK Imaging

We first detected κ And b using AO188 coupled with HiCIAO on Subaru Telescope on January 1, 2012, as part of the SEEDS survey (Tamura 2009). The observations used a $20'' \times 20''$ field of view, 9.5 mas pixels, and an opaque $0''.6$-diameter coronagraphic mask, which helped keep the saturation radius $< 0''.5$. The images were taken in the near infrared (H-band, 1.6 μm), where young substellar objects are expected to be bright with thermal radiation (Baraffe et al. 2003). Pupil tracking was used to enable angular differential imaging (ADI; Marois et al. 2006).

Data reduction of the 46 exposures of 5 s revealed, at 23 σ confidence, a pointlike source at $1''.07$ separation. Follow-up observations in J (1.3 μm; 177 exposures of 10 s), H (1.6 μm; 171 exposures of 8 s), and $K_{\rm s}$ (2.2 μm; 135 exposures of 10 s), collected on July 8–9, 2012, using the same observing setup, re-detected the source at 6, 28, and 49 σ confidence levels, respectively. Unsaturated images of the primary, taken immediately before and after each filter's observing sequence, and using a neutral density filter (0.866% for H, 1.113% for $K_{\rm s}$, and 0.590% for J) provided photometric calibration.

To optimize the ADI technique, we first reduced the data using a locally optimized

combination of images algorithm (LOCI; Lafrenière et al. 2007). HiCIAO observations of M5, combined with distortion-corrected images obtained with the Advanced Camera for Surveys (ACS) on the Hubble Space Telescope, enabled accurate pixel scale calibration to within 0.2%; the ACS astrometric calibration was based on van der Marel et al. (2007). Figure 1 (left and middle) presents a *JHK* false-color image and corresponding signal-to-noise (S/N) map after the ADI/LOCI data reduction.

Given the relatively high S/N ratios and the known difficulties in quantifying the impact of LOCI on planet photometry and astrometry, we also performed a classical ADI reduction (Marois et al. 2006) with `mean`-based point-spread function (PSF) estimation and frame co-adding. Unsharp masking on the spatial scale of 35 pixels ($\approx 7\,\mathrm{FWHM}$) was applied to the final image to flatten the residual background. The planet signal was recovered with S/N ratios comparable (within 10%) to the LOCI reduction for all the July data sets. For the somewhat lower quality January data, the measured S/N reduced from about $23\,\sigma$ to $7\,\sigma$.

To achieve unbiased photometry and astrometry, we extracted the combined κ And PSF (S/N > 1000) from the neutral density images, and placed it on an empty image frame at the location of κ And b. Applying the same unsharp masking and ADI reduction to this data as we did for the science data, we simulated the parallactic angle evolution, as recorded in the science frames. The resulting processed PSF acted as the photometric and astrometric reference for κ And b. The only non-linear step in this process was the `median`-based unsharp masking, but the large spatial scale ($\approx 7\,\mathrm{FWHM}$) ensured that subtraction effects were minimal.

We calibrated the astrometry by cross-correlating the κ And b signal with the processed calibration PSF. We estimated the uncertainty in the κ And b center to be $FWHM/(S/N)$, following Cameron et al. (2008). The uncertainties in the final relative

astrometry were dominated by our ability to determine the host star center, which was carried out through Moffat fitting of each individual exposure. We conservatively estimated the uncertainty of the Moffat fit at 0.75 pixels (7 mas). For confirmation, we applied Moffat fitting and peak fitting to unsaturated data of κ And and found that the methods agreed at the $0.5\,\sigma$ level. The photometric uncertainties were calculated as a combination of (1) representative noise in an annulus, centered on the host star, with a radius equal to the companion, (2) photometric variability in the neutral density calibration images, which yielded effective accuracies of 7–11% for the combined datasets, and (3) uncertainties in the *JHK* magnitudes of κ And.

2.2. Subaru IRCS/AO188 L' Imaging

On July 28, 2012, we followed the *JHK* observations with L'-band observations ($3.8\,\mu$m; 50 exposures of 30 s) using AO188 coupled with the Infrared Camera and Spectrograph on Subaru Telescope. We employed a $10\farcs5 \times 10\farcs5$ field of view, 20.6 mas pixel scale and no coronagraph. The host star saturated out to $\sim 0\farcs1$. The dithered observations, carried out in ADI mode, were divided into two identical sequences bracketing observations of the star HR 8799, which provided the photometric calibration (Marois et al. 2008). Observations of a third star, S810-A, were collected before the science observations as a secondary calibration check (Leggett et al. 2003).

We sky-subtracted each image using a median combination of frames taken at the other dither positions. To help maximize the high-contrast sensitivity, we processed the data using an "adaptive" LOCI process (A-LOCI; Currie et al. 2012). We also employed a moving pixel mask, where the LOCI algorithm is prevented from using, in PSF construction, pixels lying within the subtraction zone (see Lafrenière et al. 2007 for details). Figure 1 (right) shows the final image.

To quantify the κ And b throughput, we used fake point sources added to the image and processed with the same algorithm settings. As an additional check on our flux calibration, we determined the relative brightness between the HR 8799 bcd planets (all detected at S/N $>$ 7–10) using identical procedures, and confirmed its agreement with published values (Currie et al. 2011). The independent calibrations all yielded self-consistent results, ensuring confidence in the 22 σ detection of κ And b in L'. As a final check, we re-processed the L'-band data using a more classical ADI method, similar to that described for the JHK data set, and achieved consistent results. While the July L' astrometry was consistent with the July JHK results, we refrained from including it in our proper motion analysis, due to our possession of poorer-quality astrometric calibration.

3. Host Star Properties

κ And is a B9 IV star (Wu et al. 2011) located at a distance of 52.0 pc (Perryman et al. 1997). Fitzpatrick & Massa (2005) report a temperature of 11,400 $\pm$ 100 K with a sub-solar metallicity of [Fe/H] = -0.36 ± 0.09, while independent measurements by Wu et al. (2011) report values of 10,700 $\pm$ 300 K and -0.32 ± 0.15. Given the star's spectral classification, the measured low metallicity is likely due to the details of the star's accretion and atmospheric physics, as opposed to a true, initial, low metallicity (Gray & Corbally 2002). We estimate a mass of 2.4–2.5 $M_{\odot}$ using the published temperature and evolutionary tracks from Ekström et al. (2012). Table 1 summarizes the host star properties.

Zuckerman et al. (2011) proposed κ And to be a member of the $\sim$30 Myr old Columba association. To further investigate κ And's likely membership in Columba we: (1) independently calculated its Galactic kinematics from astrometry available in the literature (Perryman et al. 1997; Zuckerman et al. 2011) and compared these to the young local associations reported in Torres et al. (2008), and (2) calculated its membership probability

in these associations using the Bayesian methods of Malo et al. (2012). Our analyses showed that the star's kinematics imply a >95% probability of the star being part of the Columba association.

As an additional check, we compared the κ And$B-V$ color and absolute V magnitude (Perryman et al. 1997; van Leeuwen 2009) with members of clusters and associations with ages ranging from ∼15–700 Myr. These include Lower Centaurus Crux, α Per, Pleiades, Coma Ber, Hyades, Praesepe, and young local associations (Torres et al. 2008; van Leeuwen 2009). The color–magnitude analysis showed that κ And is consistent with other early-type stars having ages ∼20–120 Myr. The results of our analyses are consistent with the conclusions reported in Zuckerman et al. (2011); κ And's age range and kinematics suggest it is a member in the Columba association. We therefore adopt a system age of 30^{+20}_{-10} Myr (following Marois et al. 2010) for all subsequent analyses.

4. Results

4.1. Proper Motion Analysis

Located 52.0 pc from the Sun, κ And exhibits proper motion of 83.5 mas/yr (Perryman et al. 1997), enabling an effective test to distinguish bound companions from unrelated background stars. The κ And proper and parallactic motion translate to 76 mas (∼8 HiCIAO pixels) of net movement over the 6 month period between epochs. As shown in Figure 2, the companion exhibits common proper motion with the host star, and deviates from expected background star motion by $7\,\sigma$. In addition to this $7\,\sigma$ deviation in the magnitude of motion, the observed direction of motion and scatter in astrometry are completely inconsistent with that of a background star.

4.2. Physical Properties of κ And b

Figure 3 shows that the κ And b colors are most consistent with cloudy L dwarfs and overlap with several other benchmark exoplanets and low-mass companions, including HR 8799 bcd, AB Pic b, and 1RXS1609 b. Figure 4 compares κ And b colors and absolute magnitudes with `DUSTY` and `COND` evolutionary tracks (Baraffe et al. 2003; Chabrier et al. 2000), as well as low-mass companions around HR 8799 and AB Pic. The plots show κ And b as well situated between HR 8799 cde and AB Pic b. Its infrared colors are slightly bluer than those of typical field L dwarfs, possibly indicating a low surface gravity (Cruz et al. 2009). However, improved photometry is required to confirm whether this color deviation is real.

The estimated temperature of κ And b suggests that its atmospheric properties should align more closely with those of the DUSTY models (see discussions in Chabrier et al. 2000). In deriving a mass estimate from this track, we rely on the July H-band magnitude because (1) alternative J-band and January H-band measurements have higher uncertainties, (2) K_s-band mass estimates are more sensitive to atmospheric composition (see e.g. Janson et al. 2011), and (3) L'-band mass estimates have been less thoroughly tested with experimental data, and are more sensitive to age uncertainties for this age and magnitude range (see Chabrier et al. 2000).

Based on the July H-band magnitude of 15.2 ± 0.2, the estimated age of 30^{+20}_{-10} Myr, a parallax of 19.2 ± 0.7 (Perryman et al. 1997), and the `DUSTY` evolutionary models, we calculate a mass of $12.8^{+2.0}_{-1.0}$ $M_{\rm Jup}$ and a temperature of 1680^{+30}_{-20} K. As a consistency check, we calculate the predicted JK_sL' magnitudes based on the estimated 1680 K temperature, the 20–50 Myr system age, and the `DUSTY` evolutionary models. This yields J = 16.5–16.8, K_s = 14.2–14.4, and L' = 13.1–13.2 mags, all of which are in agreement with our measured multiband photometry. Additionally, the two epochs of H-band photometry are in

agreement with one another. Table 1 summarizes the complete properties of κ And b.

While the DUSTY models are likely the more relevant, we estimate a possible alternative mass using the COND evolutionary tracks. In this scenario, we determine a mass of $11.5^{+2.4}_{-1.2}$ $M_{\rm Jup}$ and a temperature of 1640^{+40}_{-20} K. More recent evolutionary models by Spiegel & Burrows (2012) offer alternative "Warm Start" scenarios that consider formation with lower levels of initial entropy. While these models do not consider combinations of mass and temperature similar to that of κ And b, they do predict generally higher masses than that of the DUSTY and COND models. In the case of κ And b, such models place the most probable mass at a value above the typical deuterium burning limit. While we currently adopt a nominal mass estimate of $12.8^{+2.0}_{-1.0}$ $M_{\rm Jup}$ for the analyses in this discovery paper (based on the DUSTY models), we defer a deeper investigation of companion mass for a follow-up paper, where we will focus on a more thorough comparison of multiband photometry with synthetic spectra.

4.3. Orbital Properties of κ And b

We estimate the semimajor axis of κ And b from its observed separation. Assuming a uniform eccentricity distribution of $0 < e < 1$, and random viewing angles, Dupuy et al. (2010) compute a median correction factor between projected separation and semimajor axis of $1.1^{+0.91}_{-0.36}$. Using this relation, we derive a semimajor axis of 61^{+50}_{-20} AU based on its projected separation of 55.2 AU ($1\farcs07$) in January 2012.

4.4. Possible Secondary Companions

The H-band sensitivity levels (see Section 2.1) allow us to rule out secondary companions with temperatures similar or warmer than that of κ And b, for separations

greater than 0.″9 (46 projected AU). For the κ And b separation (1.″1) and beyond, we may rule out secondary companions with masses $\geq 11.7\ M_{\rm Jup}$, assuming a 30 Myr system age and the `DUSTY` evolutionary models.

5. Discussion

κ And is the most massive star to host a directly imaged planet, or brown dwarf near the deuterium burning boundary. The mass ratio between κ And b and its host is $\sim$0.5%, similar to the $\sim$0.4% ratios of the β Pic and HR 8799 planets (Lagrange et al. 2009; Marois et al. 2008). In comparison, this value is noticeably smaller than those of reported directly imaged planets around 1RXS 1609 (Lafrenière et al. 2008) and 2M 1207 (Chauvin et al. 2004). The projected separation of κ And b is also intermediate between the two outer planets in HR 8799. The similarities between κ And b, β Pic, and HR 8799 could imply a similar formation mechanism, which may be distinct from recently discovered brown dwarf companions of approximately an order of magnitude larger mass ratios (e.g., GJ 758 B; Thalmann et al. 2009) or semimajor axes (e.g., HIP 78530 B; Lafrenière et al. 2011). Strengthening the possibility of a planet-like formation for Kap And b, theoretical models (e.g. Rafikov 2011) show that, for a minimum mass solar nebula, the region of the primordial disk where core accretion formation of giant planets can occur overlaps with the separation range of κ And b. Furthermore, this formation mechanism may be significantly enhanced for a star as massive as κ And, assuming it had a correspondingly more massive protoplanetary disk. Further studies will be needed to more stringently constrain the population properties of planets and brown dwarfs on intermediate and wide orbits.

The best-fit mass of κ And b lies just below the deuterium burning limit according to conventional evolutionary models, but may be above this limit if initial entropy at formation is lower than such models assume (Spiegel & Burrows 2012). This leads to an

ambiguity in whether the companion can be classified as an "exoplanet" by the present IAU definition. Such a classification scheme can however be misleading, given that κ And b may well have formed in the same way as previously imaged planets, regardless of whether its mass falls just below or above this limit. Indeed, radial velocity studies have shown that massive stars tend to have massive planets, sometimes with companions having masses above the deuterium burning limit (e.g. Lovis & Mayor 2007) and which apparently form a high-mass tail of a lower-mass planetary population (e.g. Hekker et al. 2008). On the other hand, formation history can be difficult to assess in individual cases. In order to avoid these uncertainties, we simply classify κ And b as a 'Super-Jupiter', which we take to mean a group of objects that includes the previously imaged planets around HR 8799 and β Pic as well as the most massive radial velocity planets, and which one might suspect have formed in a similar way to lower-mass exoplanets, but for which this has not necessarily been unambiguously demonstrated. This suggested class includes substellar objects with masses at or moderately above the deuterium burning limit, but excludes objects with orbital separations well beyond a typical disk truncation radius, or systems with mass ratios more indicative of a binary-like formation.

The authors thank David Lafrenière for providing the source code for his LOCI algorithm, the anonymous referee for useful comments, and Subaru Telescope staff for their assistance. The authors thank David Barrado and the Calar Alto Observatory staff for their efforts at carrying out supplementary observations of the host star. This work is partly supported by a Grant-in-Aid for Science Research in a Priority Area from MEXT, Japan, and the U.S. National Science Foundation under Award No. 1009203 (J.C., T.K., P.W., K.G.), 1008440 (C.G.), and 1009314 (J.W.). The authors recognize and acknowledge the significant cultural role and reverence that the summit of Mauna Kea has always had within the indigenous Hawaiian community. We are most fortunate to have the opportunity

to conduct observations from this mountain.

Facilities: Subaru (HiCIAO, IRCS, AO188).

REFERENCES

Baraffe, I., Chabrier, G., Barman, T. S., Allard, F., & Hauschildt, P. H. 2003, A&A, 402, 701

Béjar, V. J. S., Zapatero Osorio, M. R., Pérez-Garrido, A., et al. 2008, ApJ, 673, L185

Bihain, G., Rebolo, R., Zapatero Osorio, M. R., Béjar, V. J. S., & Caballero, J. A. 2010, A&A, 519, A93

Cameron, P. B., Britton, M. C., & Kulkarni, S. R. 2008, Proc. SPIE, 7015,

Chabrier, G., Baraffe, I., Allard, F., & Hauschildt, P. 2000, ApJ, 542, 464

Chauvin, G., Lagrange, A.-M., Dumas, C., et al. 2004, A&A, 425, L29

Chauvin, G., Lagrange, A.-M., Zuckerman, B., et al. 2005, A&A, 438, L29

Cruz, K. L., Kirkpatrick, J. D., & Burgasser, A. J. 2009, AJ, 137, 3345

Currie, T., Burrows, A., Itoh, Y., et al. 2011, ApJ, 729, 128

Currie, T., Debes, J., Rodigas, T. J., et al. 2012, ApJ, in press (arXiv:1210.6620)

Dupuy, T. J., Liu, M. C., Bowler, B. P., et al. 2010, ApJ, 721, 1725

Ekström, S., Georgy, C., Eggenberger, P., et al. 2012, A&A, 537, A146

Faherty, J. K., Rice, E. L., Cruz, K. L., Mamajek, E. E., & Núñez, A. 2012, AJ, submitted (arXiv:1206.5519)

Fitzpatrick, E. L., & Massa, D. 2005, AJ, 129, 1642

Gray, R. O., & Corbally, C. J. 2002, AJ, 124, 989

Hayano, Y., Takami, H., Oya, S., et al. 2010, Proc. SPIE, 7736,

Hekker, S., Snellen, I.A.G., Aerts, C., Quirrenbach, A., Reffert, S., & Mitchell, D.S. 2008, A&A, 480, 215

Hodapp, K. W., Suzuki, R., Tamura, M., et al. 2008, Proc. SPIE, 7014,

Ireland, M. J., Kraus, A., Martinache, F., Law, N., & Hillenbrand, L. A. 2011, ApJ, 726, 113

Janson, M., Carson, J., Thalmann, C., et al. 2011, ApJ, 728, 85

Janson, M., Bonavita, M., Klahr, H., Lafrenière, D., Jayawardhana, R. & Zinnecker, H. 2011, ApJ, 736, 89

Johnson, J.A., Aller, K.M., Howard, A.W., & Crepp, J.R. 2010, PASP, 122, 905

Lafrenière, D., Jayawardhana, R., Janson, M., et al. 2011, ApJ, 730, 42

Lafrenière, D., Jayawardhana, R., & van Kerkwijk, M. H. 2008, ApJ, 689, L153

Lafrenière, D., Marois, C., Doyon, R., Nadeau, D., & Artigau, É. 2007, ApJ, 660, 770

Lagrange, A.-M., et al. 2009, A&A, 493, L21

Leggett, S. K., Golimowski, D. A., Fan, X., et al. 2002, ApJ, 564, 452

Leggett, S. K., Hawarden, T. G., Currie, M. J., et al. 2003, MNRAS, 345, 144

Lloyd, J.P. 2011, ApJ 739, L49

Lovis, C. & Mayor, M. 2007, A&A, 472, 657

Malo, L., Doyon, R., Lafrenière, D., et al. 2012, ApJ, in press (arXiv:1209.2077)

Marois, C., Lafrenière, D., Doyon, R., Macintosh, B., & Nadeau, D. 2006, ApJ, 641, 556

Marois, C., Macintosh, B., Barman, T., et al. 2008, Science, 322, 1348

Marois, C., Zuckerman, B., Konopacky, Q. M., Macintosh, B., & Barman, T. 2010, Nature, 468, 1080

Mordasini, C., Alibert, Y., Benz, W., Klahr, H., & Henning, T. 2012, A&A, 541, 97

Omiya, M. et al. 2012, PASJ, 64, 34

Perryman, M. A. C., Lindegren, L., Kovalevsky, J., et al. 1997, A&A, 323, L49

Rafikov, R. 2011, ApJ, 727, 86

Skemer, A. J., Hinz, P. M., Esposito, S., et al. 2012, ApJ, 753, 14

Skrutskie, M.F. et al. 2006, AJ 131, 1163

Spiegel, D. S., & Burrows, A. 2012, ApJ, 745, 174

Tamura, M. 2009, American Institute of Physics Conference Series, 1158, 11

Thalmann, C., et al. 2009, ApJ, 707, L123

Tokunaga, A., et al., 1998, SPIE, 3354, 512

Torres, C. A. O., Quast, G. R., Melo, C. H. F., & Sterzik, M. F. 2008, Handbook of Star Forming Regions, Volume II, 757

van der Marel, R. P., Anderson, J., Cox, C., et al. 2007, Instrument Science Report ACS 2007-07, 22 pages, 7

van Leeuwen, F. 2009, A&A, 497, 209

Wahhaj, Z., Liu, M. C., Biller, B. A., et al. 2011, ApJ, 729, 139

Wu, Y., Singh, H. P., Prugniel, P., Gupta, R., & Koleva, M. 2011, A&A, 525, A71

Zuckerman, B., Rhee, J. H., Song, I., & Bessell, M. S. 2011, ApJ, 732, 61

This manuscript was prepared with the AAS LaTeX macros v5.2.

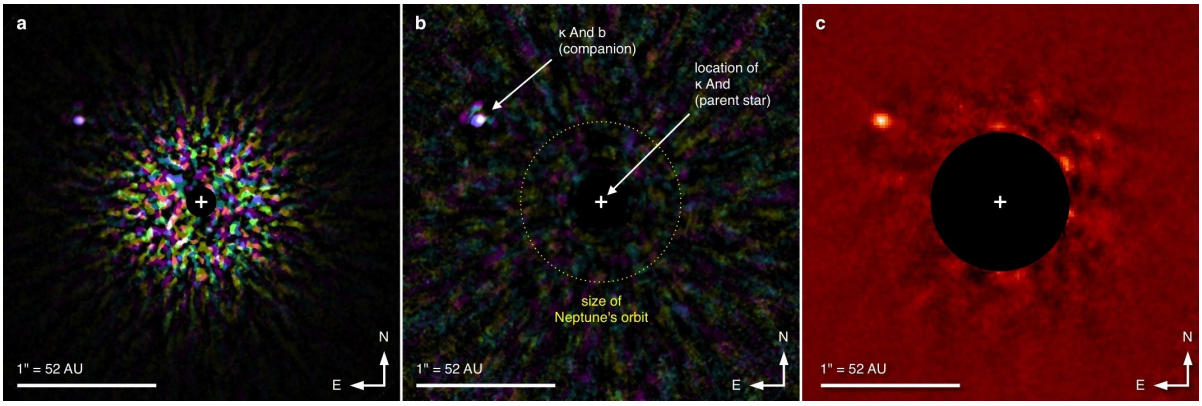


Fig. 1.— *Left*: *JHK* false-color image of κ And b after LOCI/ADI data reduction, for the 2012 July observations. *Center*: A corresponding signal-to-noise map created from the left frame. The S/N ratio is calculated in concentric annuli around the star. The white plus sign in each panel marks the location of the host star κ And; the black disks designate the regions where field rotation is insufficient for ADI. White features indicate where the signal is roughly equally strong in all wavelengths; colored features indicate where the signal is mismatched between wavelengths, and is often indicative of residual noise. The lobes around κ And b result from the Airy pattern produced by the Subaru AO188 system. *Right*: L'-band image of κ And b from the 2012 July observations.

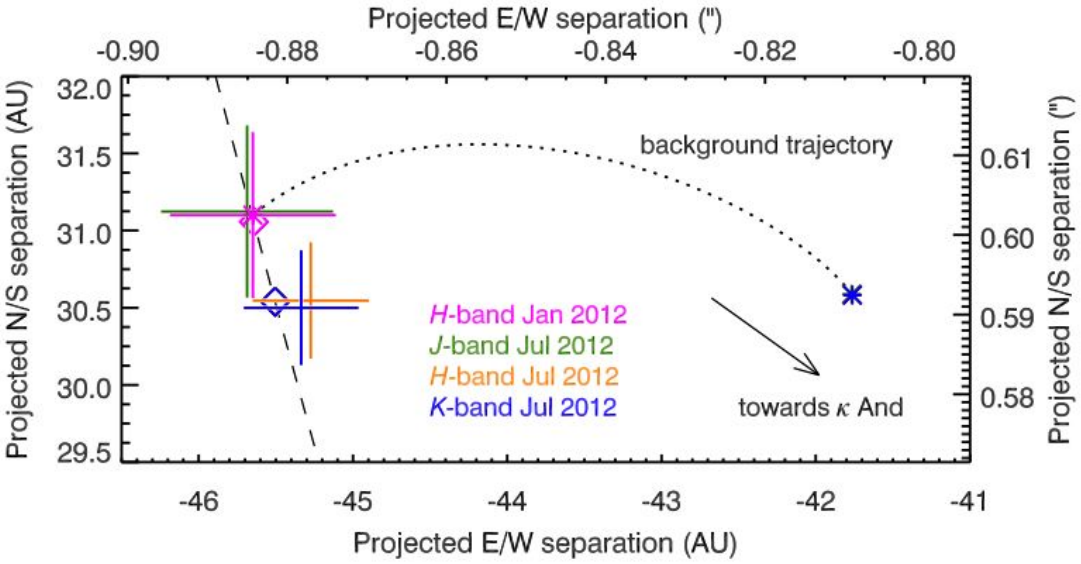


Fig. 2.— Proper-motion analysis of κ And b. The dotted curve designates the predicted parallactic and proper motion between epochs, if the detected January source were a background star. The dashed line indicates an example bound, orbital path of κ And b consistent with the observational data. The diamond symbols represent the predicted January and July astrometric measurements for κ And b, if it follows the dashed orbital path. κ And b is clearly inconsistent with background behavior and instead demonstrates common proper motion with the host star.

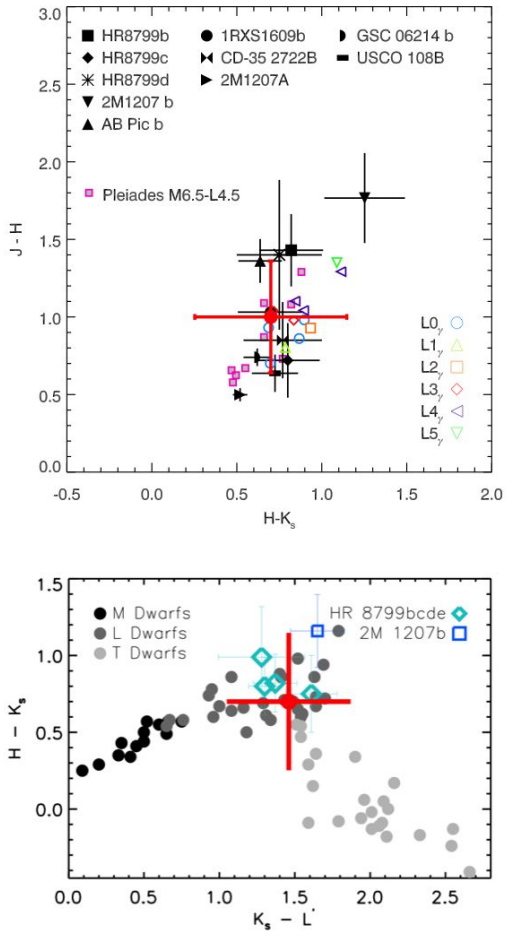


Fig. 3.— Position of κ And b colors (red points) with respect to reference objects. Top plot includes benchmark substellar companions: HR 8799 bcd (Marois et al. 2008), 2M1207 Ab (Chauvin et al. 2004), AB Pic b (Chauvin et al. 2005), 1RXS1609 b (Lafrenière et al. 2008), CD-35 2722 B (Wahhaj et al. 2011), GSC 06214 b (Ireland et al. 2011), and USCO 108 AB (Béjar et al. 2008). It also contains L dwarfs with spectral features indicative of reduced surface gravity (Cruz et al. 2009; Faherty et al. 2012), and Pleiades M-L dwarfs (Bihain et al. 2010). Bottom plot includes M, L, and T field dwarfs (Leggett et al. 2002), HR 8799 bcde (Currie et al. 2011; Skemer et al. 2012), and 2M1207 b (Chauvin et al. 2004).

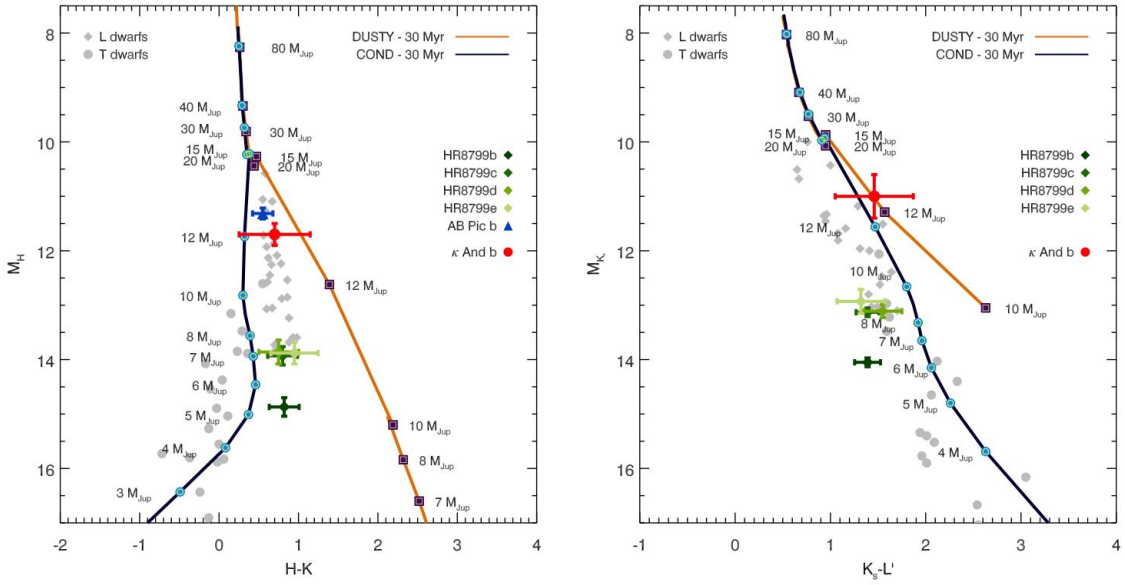


Fig. 4.— κ And b colors and absolute magnitudes (red points) compared with DUSTY and COND evolutionary tracks (Baraffe et al. 2003; Chabrier et al. 2000).

Table 1. Properties of the κ And System

Property	Primary	Companion
Mass	2.4–2.5 $M_{\odot}$ [a]	$12.8^{+2.0}_{-1.0}$ $M_{\rm Jup}$ [b]
$T_{\rm eff}$	11,400 ± 100 K [c]	$1{,}680^{+30}_{-20}$ K [b]
	10,700 ± 300 K [d]	—
Spectral Type	B9 IV [d]	L2–L8 [e]
Age (Myr)	30^{+20}_{-10} [f]	—
Parallax (mas)	19.2 ± 0.7 [g]	—
Fe/H	−0.36 ± 0.09 [c]	—
	−0.32 ± 0.15 [d]	—
$\log g$	4.10 ± 0.03 [c]	—
	3.87 ± 0.13 [d]	—
J (mag)	4.6 ± 0.3 [h]	16.3 ± 0.3
H (mag)	4.6 ± 0.2 [h]	15.2 ± 0.2
$K_{\rm s}$ (mag)	4.6 ± 0.4 [h]	14.6 ± 0.4
L' (mag)	—	13.12 ± 0.09
ΔJ (mag)	—	11.6 ± 0.2
ΔH (mag)	—	10.64 ± 0.12
$\Delta K_{\rm s}$ (mag)	—	10.0 ± 0.08
M_J (mag)	1.0 ± 0.3 [i]	12.7 ± 0.3
M_H (mag)	1.0 ± 0.2 [i]	11.7 ± 0.2
$M_{K_{\rm s}}$ (mag)	1.0 ± 0.4 [i]	11.0 ± 0.4
$M_{L'}$ (mag)	—	9.54 ± 0.09
Astrometry on 1 January 2012 (H-band):		
— Proj. sep. (″)	—	1.070 ± 0.010
— Proj. sep. (AU)	—	56 ± 2 [j]
— Position angle (°)	—	55.7 ± 0.6
Astrometry on 8 July 2012 (H-band):		
— Proj. sep. (″)	—	1.058 ± 0.007
— Proj. sep. (AU)	—	55 ± 2 [j]
— Position angle (°)	—	56.0 ± 0.4

Note. — Photometric values represent Subaru July 2012 measurements, unless noted otherwise.

[a]Calculated using the published temperature from Wu et al. (2011) and evolutionary tracks from Ekström et al. (2012).

[b]Calculated using the H-band magnitude, estimated κ And age, and evolutionary models from Chabrier et al. (2000).

[c]Fitzpatrick & Massa (2005)

[d]Wu et al. (2011)

[e]Based on measured colors and Cruz et al. (2009) spectral identifications.

[f]Zuckerman et al. (2011) and Marois et al. (2010)

[g]Hipparcos; Perryman et al. (1997)

[h]2MASS; Skrutskie et al. (2006)

[i]Calculated by the authors, using 2MASS photometry and Hipparcos parallax.

[j]Uncertainty is dominated by the host star parallax measurement.